PASTE2020 | 23rd International Conference on Paste, Thickened and Filtered Tailings

Surface Cracking in Thickened Tailings: Mechanisms and its Influence on Evaporation and Water Contents

Evelyn Arredondo*, Víctor Araya and Gonzalo Suazo
Universidad Técnica Federico Santa María, Chile

ABSTRACT

Tailings Storage Facilities (TSF) are characterized by high moisture contents of their materials even after thickening processes. After deposition the tailings undergoes to a series of phenomena such consolidation, seepage, desiccation, etc., which results in the desaturation of the pore space. The occurrence of these phenomena is influenced by several factors, such as evaporation, contraction and surface cracking. Particularly, it has been found that the surface cracking affects evaporation rates while influencing the stability of the facility due to the desaturation of deeper soil layers.

Nowadays, the assessment of water content in the field is a complex and sometimes not viable activity due to risk of personnel when moisture content is controlled manually. Knowing the moisture content can be advantageous if the stability of the facility needs to be evaluated or the water balance of the structure analyzed. So, one question that arises is: can the water content of the facility being indirectly monitored through the observations of cracks?

The latter is explored in this article by conducting desiccation tests in paste tailings under temperature and field conditions of northern Chile. The slurry is desiccated until the shrinkage limit is exceeded while RGB images captured periodically and rated of evaporation monitored. The images are then processed utilizing segmentation, linear filtering, and thresholding techniques. The processed images of the laboratory samples are then compared with images captured by unmanned aerial vehicle (UAV) in a paste storage facility. Finally an index that correlates cracking and moisture content is proposed. In addition to this, a new approach to estimate shrinkage limit is proposed.

INTRODUCTION

One of the main challenges of the mining industry in Chile consists on the efficient use of water resources, especially in the north and center regions of the country, where there is a severe scarcity of freshwater. Even though there are techniques to minimize the use of water, e.g., thickening and filtering, the water content of tailings is still high. During the operation of the tailings deposit, the water content must be continuously measured to calculate the water balance. However, the measurement in field is a complex and sometimes a hazardous task.

Once the tailings are deposited in the facility the desiccation process begins, which is dependent on its water content and ambient conditions. During desiccation, the surface of tailings cracks due to the volume contraction as the water content is reduced. It has been observed that the cracks greatly influence the evaporation rate at the onset of desaturation (Fujiyasu, Fahey, & Newson, 2000). In the same way, it has been identified that the desiccation cracks rise the hydraulic conductivity in more than one order of magnitude in comparison to samples with no cracks (Rodríguez, Candela, & Lloret, 2005). This fact has been verified by different authors (Ferrer, 2011; Konrad & Ayad, 1997; Rodríguez et al., 2007). Moreover, desiccation and shrinkage improves monotonic and seismic response of the deposit. It has been observed by the authors that the cyclic resistance ratio in paste almost double when saturation degree drops below 90%.

Surface cracking is an important factor to consider in the study of the physical and chemical stability of tailings deposits. In this work, it is explored the use of images to study the behavior of tailings in desiccation process, and the estimation of its water content. For this purpose, laboratory tests are performed to simulate the desiccation process under the same ambient conditions of the north of Chile. In these tests, the evaporation rate and the water content are continuously measured. The whole process is monitored by images in the visible spectrum range (VIS). The images are processed and two indexes are proposed to estimate the surface water content from the cracking pattern. The evaporation rates are analyzed in function of the water content, verifying its relation with the air entry-value (AEV) and the shrinkage limit (SL). Regarding the latter, a methodology is developed for calculating the SL from the shrinkage curve of the tailing, considering that the soil reaches the SL in a partially saturated state. To verify this, the results are compared to field data and images taken with an unmanned aerial vehicle (UAV).

TAILINGS BEHAVIOR POST-DEPOSITION

Once the tailings are deposited, a series of processes begin, which progressively reduce their void ratio: settling, consolidation and desiccation (Simms, Dunmola, & Fisseha, 2009). Settling is defined as the first settlement process when there is no effective stress. In this process, heavier particles descend and water tends to remain on its surface, forming a supernatant layer. Consolidation is a time-dependent process, in which the volume of the soil is reduced, as the effective stress increases through the dissipation of excess pore pressure. Desiccation is the process in which the water content of the tailings is progressively reduced, and the consolidation is increased further. From there, it is

considered that the consolidation and desiccation processes are greatly related between them, and regulated by the surface evaporation rate.

Under the previous processes, the tailings change from a saturated to a partially saturated state, that is, negative pressures or suction are developed in the porous phase of the soil. In Figure 1 a qualitative diagram of the desiccation process is shown, modified from Konrad & Ayad (1997). In this diagram, a vertical contraction takes place at the onset of desiccation, with no horizontal or radial contractions. At a certain value of suction (ψ_{cr}) the first crack is developed and from there the horizontal contraction increases. Secondary cracks are developed between two main cracks if the distance is large enough to mobilize soil resistance.

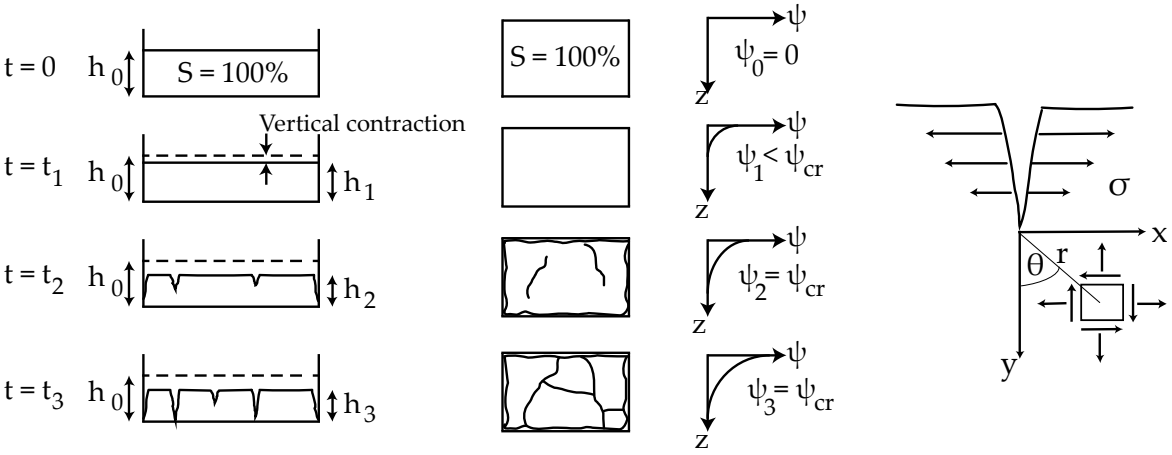

Figure 1 Schematic illustration of cracking. Modified of Konrad & Ayad (1997)

MATERIALS AND METHODOLOGY

Characterization

Index properties

The soil used in this study corresponds to a thickened tailing from an iron mine located in northern Chile. The sample if a full stream tailings, corresponding to a low plasticity clay, with the following properties: liquid limit (LL) 23.2%, plastic limit (PL) 10.7%, plasticity index (PI) 12.5%, water saturation (ws) 32%, specific gravity (Gs) 3.02, passing #200 86.5%, USCS classification CL. The granulometric curve and water retention curve (SWRC) are shown in Figure 2.

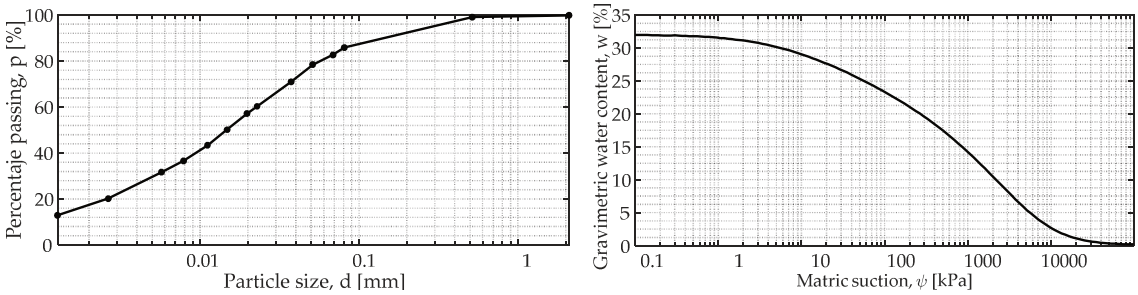

Figure 2 Tailing particle size distribution (left) and water retention curve (right)

Shrinkage limit (SL)

The shrinkage limit (SL) of the soil was carefully determined in this study as it plays a key role on the understanding of shrinkage behavior. The SL was calculated according to ASTM D 4943 – 02, for initial solid contents (SC) of 80%, 70% and 66%, obtaining values for SL of 19.6%, 22.3% and 26.2%, respectively. However, these values are very close to the LL and greater to the PL of the soil. Thus, tests were carried out to determine the shrinkage curve of the soil, studying its behavior in the complete range of water contents. During the tests, the volume and weight of the samples were periodically measured for 7 days. Circular containers of 5 cm in diameter and 1.5 cm in height were utilized. The dimensions of the containers were selected to avoid the cracking of the soil during desiccation. The samples were prepared with solid contents of 80%, 70% and 64%, and slowly poured in the containers, ensuring the complete saturation at the beginning of the test. The obtained results for the void ratio were fitted according to Equation (1), introduced by Fredlund (1999) and utilized by Zhang et al. (2018).

$$e(w) = a_{sh} \cdot \left[\left(\frac{w}{b_{sh}}\right)^{c_{sh}} + 1\right]^{\frac{1}{c_{sh}}} \tag{1}$$

Where: a_{sh} is the minimum void ratio (e_{min}), a_{sh}/b_{sh} is the slope of the asymptotic line, c_{sh} is the curvature of the shrinkage curve, and a_{sh}, b_{sh}, c_{sh} are fitting parameters of the shrinkage equation.

The obtained void ratio versus gravimetric water content is shown in Figure 3, noting that the greater is the SC, the lower is the final void ratio. However, all the samples followed the same asymptotic line before reaching the SL, regardless SC.

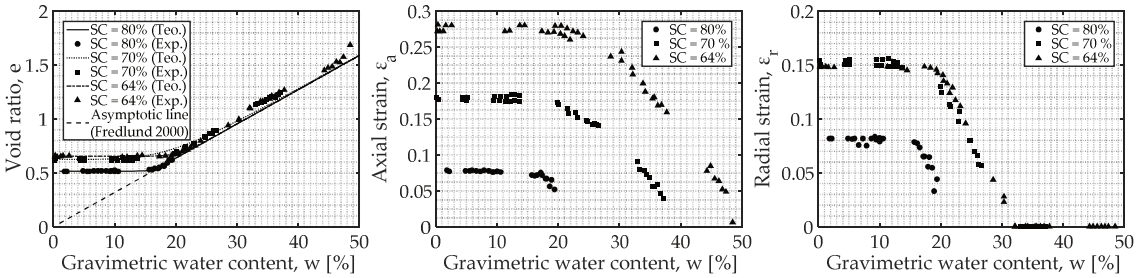

Figure 3 Void ratio versus gravimetric water content (left), axial strain versus gravimetric water content (center), and radial strain versus gravimetric water content (right)

The obtained axial and radial strain versus gravimetric water content are shown in Figure 3. As can be seen, the axial strain begins to increase at higher levels of water content in comparison to the radial strain. However, the radial strain continues to increase even though the axial strain halted. Due to this, it is possible to define the SL of the tailing here as the value of water content in which the radial strain halts. Consequently, for an SC of 70% the SL is 19%. The discrepancy in the values of SL concerning ASTM D4943 – 02 is because the latter assumes the soil reaches the SL in a 100% degree of saturation, which is not strictly true. In the laboratory tests, it was observed that the soil reaches the SL with a degree of saturation in a range of 80% to 95%.

Experimental setup

For the desiccation test, a two-level metallic structure was built. The samples were placed at the bottom level, while the instruments, such as the camera and fans, are placed in the upper level. The soil was prepared in a saturated state, with an SC of 70%. The desiccation pans utilized were flat squared sized (20x20 cm). Eight tests were carried out, with an area to height ratio (AHR) between 100cm²/cm and 800 cm²/cm. The potential evaporation (PE) was periodically measured. In the Figure 4 a diagram of the experimental setup is shown.

The field conditions were simulated using 250W IR lamps and 5W fans, reaching an average of 35°C. The ambient humidity was not registered, because according to the results of Rodríguez (2002) this factor does not affect the cracking pattern. Nevertheless, humidity in the Laboratory was steady. Water evaporation was measured as the weight loss of the pans during the desiccation. When the first cracks developed, the lamps and fans were turned off to slow the cracking. The desiccation progress was continuously monitored with cameras in the visible-light spectral range (VIS). The tests end when there is no visible change in the volume of the samples, i.e., when there is no change in vertical and horizontal strain.

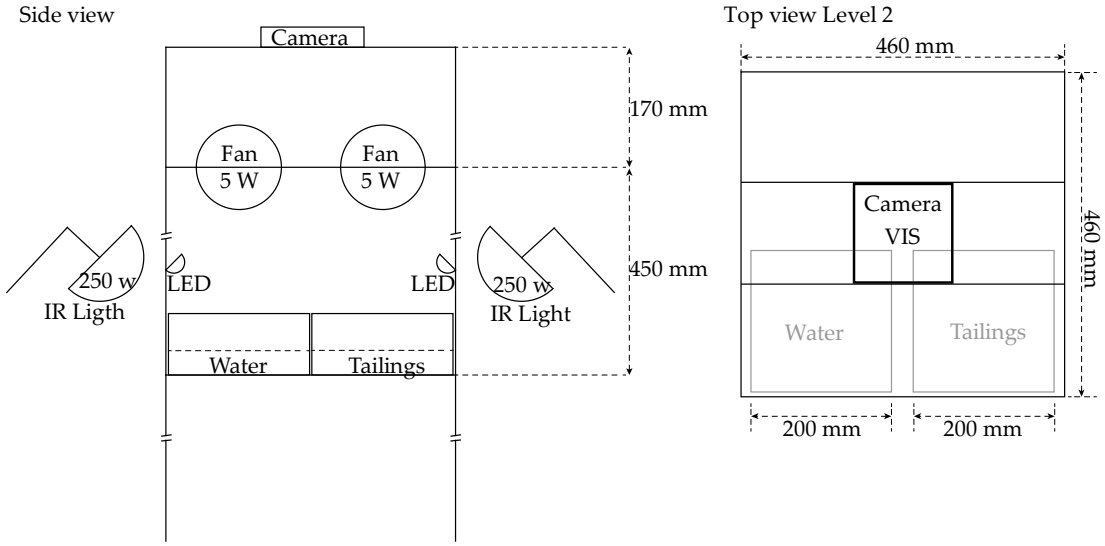

Figure 4 Experimental setup implemented in laboratory

Field investigation

Due to the large surface of tailings deposits, the fresh upper layers are of low height, in a range of 30 cm to 60 cm. Therefore, the AHR tends to be high, generally, AHR > 400 cm²/cm. For this reason, to study the effect of AHR in the cracking pattern, eight tests of desiccation with AHR in the range of 100 cm²/cm y 800 cm²/cm are performed.

The cracking pattern of the samples was compared with images of a tailings deposit located in northern Chile. The images of the surface of the deposit were taken with a UAV from a height of 50 m, in the VIS and RGB format, with a resolution of 4864 by 3648 pixels.

Digital image processing

The analysis of the images obtained in the laboratory test was done through segmentation techniques, utilizing the open-source software ImageJ. The RGB images were converted to gray scale, simplifying the segmentation. The objective of the analysis was to separate the cracked from the non-cracked area, generating a binary mask. For this reason, two properties were studied: isolated points, lines and edges detection; gray-tone similarity, for region segmentation by division and fusion, and growing and thresholding. The proposed indexes, as discussed later in the present paper, were calculated from the thresholding applied to each image.

RESULTS AND DISCUSSION

Cracking pattern and AHR

In Figure 5 at the top, three of the obtained cracking pattern in laboratory tests are shown, while at the bottom the cracking patterns of the tailings deposit are shown. As can be seen, the cracking pattern was successfully reproduced in the laboratory, with the selected AHR. Specifically, it was observed that in all the tests the first crack developed in a partially saturated state, near the 80%-85% of saturation, and with water content close to the LL of the soil. Geometrically, as the AHR is increased, the width and length of the cracks tend to a constant value.

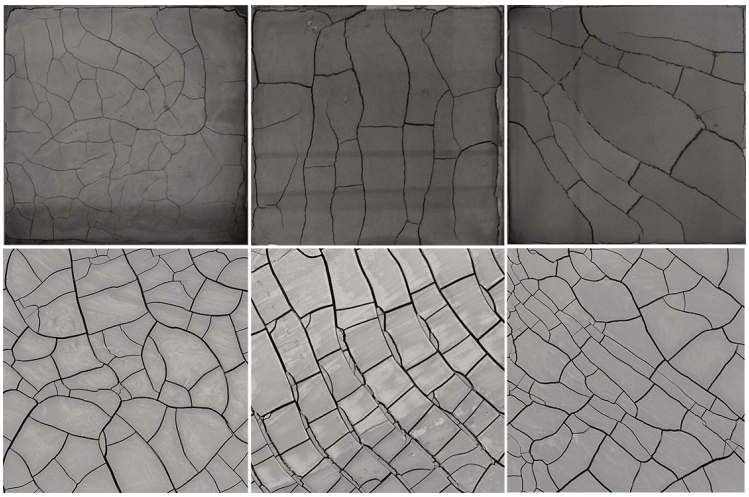

Figure 5 Laboratory results at the end of desiccation (top), and cracking patterns of the tailings deposit (bottom)

Relation between water content and cracking pattern

The digital image processing separates in a binary mask the cracked and the non-cracked background areas of the surface of the tailing. In this way, a matrix is obtained with values of 0 to represent the background in black color, and 255 to represent the cracks in white color. Under the hypothesis of a correlation between the water content and the crack development, two indexes are proposed. The proposed index I represents the percentage of cracked area, defined in Equation (2), while the index II as the ratio between the number of blocks and the total area, as is shown in Equation (3).

$$I_1 = \frac{number\ of\ white\ pixels}{Total\ number\ of\ pixels} \tag{2}$$

$$I_2 = \frac{number\ of\ polygonal\ blocks}{total\ area} \tag{3}$$

In Figure 6 the image processing for one of the tests, and at the end of the cracking process, is shown. At left an image in gray-scale is illustrated, while at the center the resulting binary mask is presented. At the right, the identification of polygonal blocks for the same test is shown.

Figure 6 Image processing: gray scale image (left), binary mask (middle), and polygonal blocks (right)

Quantitatively, each index represents the level of surface cracking for certain water content, and therefore for higher index values the level of cracking is higher, and the water content is lower.

In Figure 7 the curves of indexes I and II versus water content for two tests are shown. The SL is shown as a dashed line, obtained from the shrinkage curve of the soil.

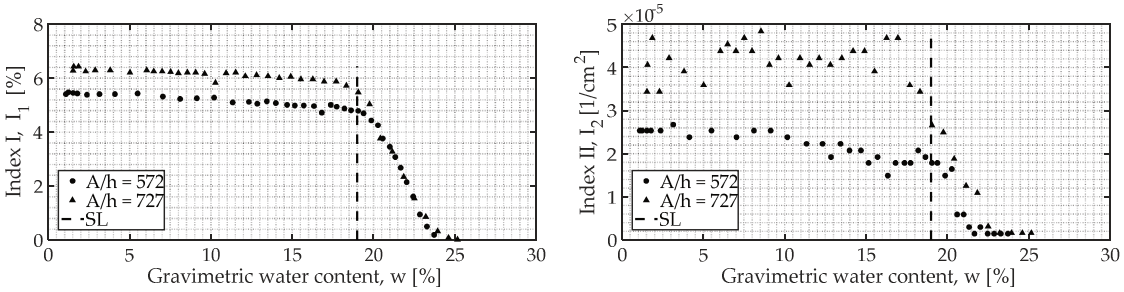

Figure 7 Gravimetric water content versus Index I (left), and gravimetric water content versus Index II (right)

By definition, the index I is greater than zero as the first crack is developed. As can be seen in Figure 7 at left, the first crack develops when the water content is close to the 24% for both tests, i.e., the surface cracks when the humidity is close to the LL of the soil, independently of its AHR. It is observed that both indexes follow the same initial slope in the two samples, and once the SL is reached, they tend to a constant value.

Evaporation rates

The evaporation rate normalized by the PE for the two of the performed tests is shown in Figure 8. In the same graphs the air entrance value (AEV), the water content when the first crack develops, and the SL value are highlighted. These values define four stages in the desiccation of the tailing. The first stage presents a high evaporation rate at the beginning of the desiccation, due to the high water content, forming a thin layer of water at the surface. As this layer of water drops down owing to evaporation, the evaporation rate remains approximately constant until the AEV is reached, in which

the soil changes to a partially saturated state (S < 100%). The second stage corresponds to a water content in the range between the AEV and the first crack development. In this stage, the soil exhibits only vertical contraction, and the saturation degree decreases gradually as the evaporation rate slowly increases in comparison to the previous stage. The third stage is defined between the first crack development and the SL. A further increase in the evaporation rate is experienced from the previous stage. This is explained by the additional evaporation through the vertical exposed areas of the cracks. Finally, a fourth stage is defined from the SL to the end of the test. In this stage, the water content of the samples is lower than 15% with no increase in surface cracking, and therefore the evaporation area remains constant. Due to this fact, the evaporation rate falls as the water content decreases. Even though the four stages are identified, oscillations in the evaporation rate are experienced, which are attributed to laboratory ambient effects.

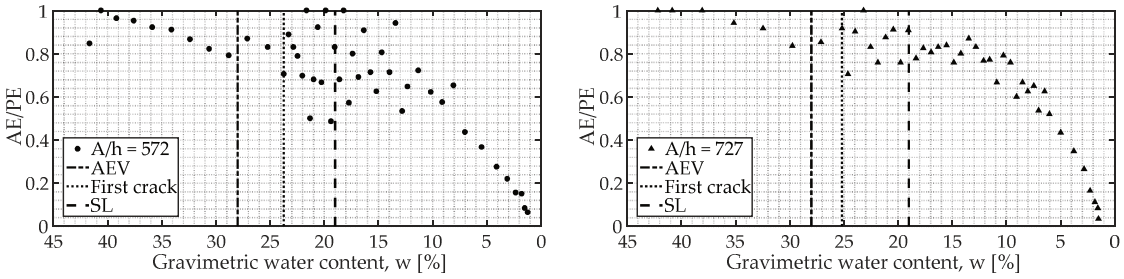

Figure 8 Gravimetric water content versus evaporation

CONCLUSION

Based on the results obtained, a relation between the AHR and the cracking pattern is proposed. And thus, a relation between the cracking pattern, the water content and the evaporation rates do exist and it is observed in this study. The results prove that the cracking of the tailings is related with different parameters such as the LL, SL and AEV, which defines four stages in the desiccation process. Besides, the SL obtained from the shrinkage curve agrees with the curves of both proposed indexes. Additionally, it was verified that the tailings reached the SL in a partially saturated state.

Due to the above, it is determined the optimum condition for tailing deposition, which takes place once the deposited layer has reached the SL. The SL can be identified from the proposed indexes, where the latter are calculated from the capture of aerial images of the surface.

The future work includes the proposal of fitting functions for the shrinkage curve with respect to the axial and radial strains. Additionally, the influence of various factors, e.g., the SC, fine content and initial soluble salt concentration on the cracking pattern will be studied further. The laboratory results will be compared with field measurements of tailings deposits from the north of Chile. To verify the proposed indexes, regarding that iron tailings have different behavior from other tailings such as copper tailings, the tests will be repeated on other facilities.

The implementation of the technique presented herein would be suitable for optimizing disposal of tailings (e.g. to decrease wind erosion or water consumption) contributing to mining sustainability.

ACKNOWLEDGEMENTS

The authors would like to acknowledge the support provided by Universidad Técnica Federico Santa Maria and the company GeoTailings Consulting (www.geotailings.cl).

REFERENCES

Ferrer, G. (2011). *Estudio del comportamiento sísmico de relaves espesados mediante el análisis de columna unidimensional, considerando grietas de contracción*. Pontificia Universidad Católica de Chile - Escuela de Ingeniería.

Fredlund, M. D. (1999). *The Role of Unsaturated Soil Property Functions in the Practice of Unsaturated Soil Mechanics*.

Fujiyasu, Y., Fahey, M., & Newson, T. (2000). Field Investigation of Evaporation from Freshwater Tailings. *Journal of Geotechnical Engineering*, *126*(June), 556–567.

Konrad, J.-M., & Ayad, R. (1997). An idealized framework for the analysis of cohesive soils undergoing desiccation. *Canadian Geotechnical Journal*, *34*(4), 477–488. https://doi.org/10.1139/t98-070

Rodríguez, R., Candela, L., & Lloret, A. (2005). Experimental System for Studying the Hydromechanical Behavior of Porous Media. *Vadose Zone Journal*, *4*(2), 345. https://doi.org/10.2136/vzj2004.0105

Rodríguez, R., Sánchez, M., Ledesma, A., & Lloret, A. (2007). Experimental and numerical analysis of desiccation of a mining waste. *Canadian Geotechnical Journal*, *44*(6), 644–658. https://doi.org/10.1139/t07-016

Simms, P., Dunmola, A., & Fisseha, B. (2009). Generic predictions of drying time in surface deposited thickened tailings in a "wet" climate. *Tailings and Mine Waste*, 749–758.

Zhang, M. F., Wilson, W. G., & Fredlund, D. G. (2018). Abstract : *Canadian Geotechnical Journal*, *55*(2), 191–207.